CONEM 2016
CONGRESSO NACIONAL DE ENGENHARIA MECÂNICA
21 - 25 AGOSTO DE 2016
FORTALEZA - CEARÁ

PHENOMENOLOGICAL MODELING OF THE THERMO-MAGNETO-MECHANICAL BEHAVIOR OF MAGNETIC SHAPE MEMORY ALLOYS

Vandré F. De Souza, vandreufrj@gmail.com[1]
Marcelo A. Savi, savi@mecanica.ufrj.br[1]
Alberto Paiva, paiva.ufrj@gmail.com[2]
Luciana L. Silva, lucianals@lts.coppe.ufrj.br[3]

[1] Universidade Federal do Rio de Janeiro
COPPE – Department of Mechanical Engineering
Center for Nonlinear Mechanics
21.945.970 – Rio de Janeiro – RJ – Brazil

[2] Universidade Federal Fluminense - Escola de Engenharia Industrial Metalúrgica de Volta Redonda
27.255.250 −Volta Redonda − RJ − Brazil

[3] CEFET/RJ - Department of Mechanical Engineering
20271-110 – Rio de Janeiro − RJ − Brazil

Abstract. *Magnetic shape memory alloy (MSMA) is a smart material that offers fast actuation and contactless control of large deformation. This paper deals of a new constitutive model based on internal variables that describes the characteristics of the phenomenological behavior of MSMA. Four macroscopic phases are considered representing austenite and three variants of martensitic phase. A numerical procedure is proposed to deal with the nonlinearities of the model. Model predictions are presented for different loadings, including magnetic field induced phase transformations (FIPT) and magnetic field induced reorientation (MFIR). Model capabilities are investigated considering numerical simulations. A comparison with experimental data of FIPT and MFIR available in literature attests the model ability to capture the general thermo-magneto-mechanical behavior of MSMA.*

Keywords: *Magnetic shape memory alloys, Constitutive modeling, Reversible magnetic shape memory effect, Magnetic field-induced phase transformation Magnetic field-induced reorientation*

1. INTRODUCTION

The so-called smart materials have increasingly importance on the design of new adaptive mechanical systems. This adaptive behavior allows the modification of form or physical properties by imposing electric or magnetic fields, as well as changing its temperature or stress. In this regard, magnetic shape memory alloys (MSMA) have emerged as an interesting alternative of this class of materials presenting the ability to convert magnetic energy into mechanical energy.

MSMA appeared in 1996 (Ullakko *et al*., 1996) when Ni_2MnGa single crystals presented a strain of 0.2% under a moderate field of 1T. These alloys exhibit an interesting combination of elastic and magnetic properties that can be observed by applying a magnetic field. The observed Magnetic-Field-Induced Strain (MFIS) has the same order as the highest magnetostriction obtained in magnetostrictive materials such as $Tb_{0.27}Dy_{0.73}$ and Terfenol-D (Ullakko *et al*., 1996). New materials as NiMnGa started presenting strain levels of 6-10% (Murray *et al*., 2000; Tickle and James, 1999) introducing new perspectives of the production of power and motion, combining advantages of traditional SMA characteristics with large frequencies to 1–2 kHz in the presence of moderate magnetic fields (Henry *et al*., 2002).

Several research efforts are focused on the description of the magnetic field-induced strain of NiMnGa due to the martensitic reorientation. Different aspects of the material behavior have been emphasizing micromagnetic models that are focused on the fundamental mechanism in microscopic scale (James and Wuttig, 1998). Phase-field models established different order parameters providing descriptions of the evolutions of magnetic domains and martensitic microstructures (Jin, 2009; Li *et al*., 2011). Phenomenological models based on thermodynamic principles were proposed considering internal variables that represent the main features of the material behavior (Kiefer and Lagoudas,

2005).

According to Liang *et al*. (2003), the complexity of the development of mechanical devices with magnetic shape memory alloys is in obtaining accurate models for these materials, since their behavior is characterized by large strains and nonlinearities. Therefore, to explore the full engineering potential of MSMA, a comprehensive model is required so that the materials' behavior may be reliably predicted.

Motivated by the promising characteristics of MSMA, this article deals with a new constitutive model based on internal variables that describes the phenomenological behavior of MSMA. The idea is to describe the general thermomechanical behavior of SMAs, incorporating the magnetic field induced phase transformation (FIPT) and the magnetic field induced martensitic variant reorientation, usually called magnetic field induced strain (MFIS). Model verification is carried out comparing numerical results with experimental data available in the literature.

2. CONSTITUTIVE MODEL

The model proposed in this paper is based on a shape memory alloy (SMA) model with internal constraints (Paiva *et al*., 2005) that considers four macroscopic phases representing austenite and three variants of martensite. The original model was originally employed for the description of classical SMAs (Savi *et al*., 2002; Baêta-Neves *et al*., 2004 and Paiva & Savi, 2005). This work presents a new thermo-magneto-mechanical version of this model, where the introduction of a magnetic term allows on to coherently describe phase transformations induced by stress, temperature and magnetic field, capturing the main features of the thermo-magneto-mechanical behavior of MSMA.

In order to describe the behavior of MSMA, Helmholtz free energy density, ψ, is adopted for each macroscopic phase. Four phases are adopted for the material description: $\mathcal{M}$, corresponding to twinned martensite; $\mathcal{M}^+$, associated with tensile detwinned martensite; $\mathcal{M}^-$, related to compressive detwinned martensite; and $\mathcal{A}$, representing austenite. Each free energy is a function of elastic strain, ε^e, temperature, T, $(\mathcal{A})$ and magnetization, M. Hence, the following functions are adopted:

$$\mathcal{M}^+: \rho\psi^+(\varepsilon^e, T, M) = \frac{1}{2}E^{\mathcal{M}}\varepsilon^{e2} - \alpha\,\varepsilon^e - \Lambda^{\mathcal{M}} - \Omega^{\mathcal{M}}(T - T_0)\varepsilon^e \tag{1}$$

$$\mathcal{M}^-: \rho\psi^-(\varepsilon^e, T, M) = \frac{1}{2}E^{\mathcal{M}}\varepsilon^{e2} + \alpha\,\varepsilon^e - \Lambda^{\mathcal{M}} - \Omega^{\mathcal{M}}(T - T_0)\varepsilon^e \tag{2}$$

$$\mathcal{A}: \rho\psi^{A}(\varepsilon^e, T, M) = \frac{1}{2}E^{\mathcal{A}}\varepsilon^{e2} - \Lambda^{\mathcal{A}} - \Omega^{\mathcal{A}}(T - T_0)\varepsilon^e + \mu_0 H M^{\mathcal{A}} \tag{3}$$

$$\mathcal{M}: \rho\psi^{\mathcal{M}}(\varepsilon^e, T, M) = \frac{1}{2}E^{\mathcal{M}}\varepsilon^{e2} + \Lambda^{\mathcal{M}} - \Omega^{\mathcal{M}}(T - T_0)\varepsilon^e + \mu_0 H M^{\mathcal{M}} \tag{4}$$

In the previous equations, superscript $\mathcal{M}$ is related to martensitic phase while subscript $\mathcal{A}$ is associated with austenite. Observing these indexes, one can define the following parameters: α is related to the stress–strain hysteresis loop height observed during the martensitic transformation; H is the magnetic field, while E represents the elastic modulus, Ω is related to the thermal expansion coefficient; $\Lambda = \Lambda(\mathrm{T})$ are temperature functions related to the phase transformation; T_0 is a reference temperature for which the material is in a stress-free condition; ρ is the density, and μ_0 is the permeability.

In order to describe mixture behavior, it is necessary to defined volume fractions of each phase: $\beta^{\mathcal{M}}$, β^+, β^- and $\beta^{\mathcal{A}}$ respectively related to $\mathcal{M}$, $\mathcal{M}^+$, $\mathcal{M}^-$ and $\mathcal{A}$. Hence, the free energy for the mixture can be written as:

$$\rho\tilde{\psi}(\varepsilon^e, T, M, \beta^+, \beta^-, \beta^{\mathcal{A}}, \beta^{\mathcal{M}}) = \rho(\beta^+\psi^+ + \beta^-\psi^- + \beta^{\mathcal{A}}\psi^{\mathcal{A}} + \beta^{\mathcal{M}}\psi^{\mathcal{M}}) + \hat{J}(\beta^+, \beta^-, \beta^{\mathcal{A}}, \beta^{\mathcal{M}}) \tag{5}$$

where $\hat{\mathrm{J}}(\beta^+, \beta^-, \beta^{\mathcal{A}}, \beta^{\mathcal{M}})$ represents an indicator function related to the coexistence of four distinct phases, which is represented by constraints related to the convex set:

$$\Theta = \{\beta^m \in \Re | 0 \le \beta^m \le 1 (m = +, -, \mathcal{A}, \mathcal{M});\ \beta^+ + \beta^- + \beta^{\mathcal{A}} + \beta^{\mathcal{M}} = 1\} \tag{6}$$

According to the above restriction, it is possible to eliminate one of the volume fractions: $\beta^{\mathcal{M}} = 1 - \beta^+ - \beta^- - \beta^{\mathcal{A}}$, making it possible to define a free energy as a function of only three internal variables $(\beta^+, \beta^-, \beta^{\mathcal{A}})$.

$$\begin{aligned}\rho\tilde{\psi}(\varepsilon^e, T, H, \beta^+, \beta^-, \beta^{\mathcal{A}}) = {} & \rho\{\beta^+[-\alpha\,\varepsilon^e - \Lambda - \mu_0 H M^{\mathcal{M}}] + \beta^-[\alpha\,\varepsilon^e - \Lambda - \mu_0 H M^{\mathcal{M}}] + \\ & + \beta^{\mathcal{A}}\left[\frac{1}{2}(E^{\mathcal{A}} - E^{\mathcal{M}})\varepsilon^{e2} + \Lambda^{\aleph} - (\Omega^{\mathcal{A}} - \Omega^{\mathcal{M}})(T - T_0)\varepsilon^e + \mu_0 H(M^{\mathcal{A}} - M^{\mathcal{M}})\right] +\end{aligned} \tag{7}$$

$$+\frac{1}{2}E^{\mathcal{M}}\varepsilon^{e2}+\Lambda_{\mathcal{M}}-\Omega^{\mathcal{M}}(T-T_0)\varepsilon^{e}+\mu_0 HM^{\mathcal{M}}\Big\}+J_{\pi}(\beta^{+},\beta^{-},\beta^{\mathcal{A}})$$

where J_π is the new indicator function of the convex set π, which establishes the constraints associated with the phases' coexistence defined as follows.

$$\pi=\{\beta^{m}\in\ \Re|0\leq\beta^{m}\leq 1(m=+,-,\mathcal{A});\beta^{+}+\beta^{-}+\beta^{\mathcal{A}}\leq 1\} \tag{8}$$

At this point, an additive decomposition is assumed so that the elastic strain may be written as:

$$\varepsilon^{e}=\varepsilon+\alpha^{h}(\beta^{-}-\beta^{+}) \tag{9}$$

where α^h is a parameter associated with the stress–strain hysteresis loop width. By replacing Eq. (9) in Eq. (7), the final form of the total free energy function becomes as follows:

$$\begin{aligned}\tilde{\psi}(\varepsilon,T,M,\beta^{+},\beta^{-},\beta^{\mathcal{A}})=\ &\rho\{\beta^{+}\left[-\alpha\left(\varepsilon+\alpha^{h}(\beta^{-}-\beta^{+})\right)-\Lambda-\mu_0 HM^{\mathcal{M}}\right]+\\&+\beta^{-}\left[\alpha\left(\varepsilon+\alpha^{h}(\beta^{-}-\beta^{+})\right)-\Lambda-\mu_0 HM^{\mathcal{M}}\right]+\\&+\beta^{\mathcal{A}}\left[\frac{1}{2}(E^{\mathcal{A}}-E^{\mathcal{M}})\left(\varepsilon+\alpha^{h}(\beta^{-}-\beta^{+})\right)^{2}+\Lambda^{\aleph}+\right.\\&\left.-(\Omega^{\mathcal{A}}-\Omega^{\mathcal{M}})(T-T_0)\left(\varepsilon+\alpha^{h}(\beta^{-}-\beta^{+})\right)+\mu_0 H(M^{\mathcal{A}}-M^{\mathcal{M}})\right]\\&+\frac{1}{2}E^{\mathcal{M}}\left(\varepsilon+\alpha^{h}(\beta^{-}-\beta^{+})\right)^{2}+\Lambda_{\mathcal{M}}-\Omega^{\mathcal{M}}(T-T_0)\left(\varepsilon+\alpha^{h}(\beta^{-}-\beta^{+})\right)+\mu_0 HM^{\mathcal{M}}\}+J_{\pi}(\beta^{+},\beta^{-},\beta^{\mathcal{A}})\end{aligned} \tag{10}$$

According to the standard generalized material formalism (Lemaitre & Chaboche, 1990), thermodynamical forces associated with each model variable are defined as follows:

$$\sigma=\rho\frac{\partial\tilde{\psi}}{\partial\varepsilon}=E\left(\varepsilon+\alpha^{h}(\beta^{-}-\beta^{+})\right)+\alpha^{h}(\beta^{-}-\beta^{+})-\Omega(T-T_0) \tag{11}$$

$$\begin{aligned}B^{+}=-\rho\frac{\partial\tilde{\psi}}{\partial\beta^{+}}=&\ \alpha\,\varepsilon+\Lambda+\beta^{-}\left(2\alpha^{h}\alpha\ +E\alpha^{h^2}\right)-\beta^{+}\left(2\alpha^{h}\alpha\ +E\alpha^{h^2}\right)+\alpha_h[E\varepsilon-\Omega(T-T_0)]\\&-\mu_0 HM^{\mathcal{M}}-\partial_1 J_{\pi}\end{aligned} \tag{12}$$

$$\begin{aligned}B^{-}=-\rho\frac{\partial\tilde{\psi}}{\partial\beta^{-}}=&-\alpha\,\varepsilon+\Lambda+\beta^{+}\left(2\alpha^{h}\alpha\ +E\alpha^{h^2}\right)-\beta^{-}\left(2\alpha^{h}\alpha\ +E\alpha^{h^2}\right)-\alpha^{h}[E\varepsilon-\Omega(T-T_0)]\\&-\mu_0 HM^{\mathcal{M}}-\partial_2 J_{\pi}\end{aligned} \tag{13}$$

$$\begin{aligned}B^{\mathcal{A}}=-\rho\frac{\partial\tilde{\psi}}{\partial\beta^{\mathcal{A}}}=&-\frac{1}{2}(E^{\mathcal{A}}-E^{M})\left(\varepsilon+\alpha_h(\beta^{-}-\beta^{+})\right)^{2}+\Lambda^{\aleph}\\&+(\Omega^{\mathcal{A}}-\Omega^{\mathcal{M}})(T-T_0)\left(+\alpha^{h}(\beta^{-}-\beta^{+})\right)-\mu_0 H(M^{\mathcal{A}}-M^{\mathcal{M}})-\partial_3 J_{\pi}\end{aligned} \tag{14}$$

$$B^{M^{\mathcal{A}}}=\frac{\rho}{\mu_0}\left(\frac{\partial\tilde{\psi}}{\partial M^{\mathcal{A}}}\right)=\ \mu_0 H\beta^{\mathcal{A}} \tag{15}$$

$$B^{M^{\mathcal{M}}}=\frac{\rho}{\mu_0}\left(\frac{\partial\tilde{\psi}}{\partial M^{\mathcal{M}}}\right)=\mu_0 H\left(-\beta^{+}\ -\beta^{-}\ -\beta^{\mathcal{A}}-1\right) \tag{16}$$

where σ represents stress and $\partial_i J_\pi$ are sub-differentials with respect to β^m (Rockafellar, 1970), responsible for ensuring the restriction associated at J_π. Lagrange multipliers offer an alternative to represent sub-differentials of the indicator function (Savi & Braga, 1993). Furthermore, parameters E and Ω can be defined from their correspondent values for austenitic and martensitic phases, as follows:

$$E=E^{\mathcal{M}}+\beta^{\mathcal{A}}(E^{\mathcal{A}}-E^{\mathcal{M}}) \tag{17}$$

$$\Omega=\Omega^{\mathcal{M}}+\beta^{\mathcal{A}}(\Omega^{\mathcal{A}}-\Omega^{\mathcal{M}}) \tag{18}$$

$$\mathbb{M}=-M^{\mathcal{M}}+\beta^{\mathcal{A}}(M^{\mathcal{A}}-M^{\mathcal{M}}) \tag{19}$$

Temperature dependent functions $\Lambda = \Lambda(T)$ and $\Lambda^{\aleph} = \Lambda^{\aleph}(T)$ define transformation critical stress, being given by the following expressions:

$$\Lambda = 2\Lambda^{\mathcal{M}} = \begin{cases} -\mathrm{L}_0 + \dfrac{\mathrm{L}}{\mathrm{T}^{\mathcal{M}}}(\mathrm{T} - \mathrm{T}^{\mathcal{M}}), & \text{if } \mathrm{T} > \mathrm{T}^{\mathcal{M}} \\ -\mathrm{L}_0\,, & \text{if } \mathrm{T} \le \mathrm{T}^{\mathcal{M}} \end{cases} \tag{20}$$

$$\Lambda^{\aleph} = \Lambda^{\mathcal{M}} + \Lambda^{\mathcal{A}} = \begin{cases} -\mathrm{L}_0^{\mathcal{A}} + \dfrac{\mathrm{L}^{\mathcal{A}}}{\mathrm{T}^{\mathcal{M}}}(\mathrm{T} - \mathrm{T}^{\mathcal{M}}), & \text{if } \mathrm{T} > \mathrm{T}^{\mathcal{M}} \\ -\mathrm{L}_0^{\mathcal{A}}, & \text{if } \mathrm{T} \le \mathrm{T}^{\mathcal{M}} \end{cases} \tag{21}$$

Since magnetic shape memory alloys have an essentially dissipative behavior, it is necessary to introduce a dissipation potential, ϕ , or its dual, ϕ^*. The form of the dual of the dissipation potential is assumed to be a function of the thermodynamic forces, as follows:

$$\phi^* = \frac{1}{2\eta^M}(B^+)^2 + \frac{1}{2\eta^M}(B^-)^2 + \frac{1}{2\eta^A}(B^{\mathcal{A}})^2 + \frac{1}{\eta^H} f\left(B^{M^{\mathcal{M}}}\right) \tag{22}$$

Therefore, it is possible to rewrite the equations of evolution for volumetric fractions as a function of the parameters of internal dissipation of the material.

$$\dot{\beta}^+ \in \partial_{\mathrm{B}^+}\phi^* = \frac{B^+}{\eta^T}, \qquad \dot{\beta}^+ \in \partial_{\mathrm{B}^+}\phi^* = \frac{B^+}{\eta^T}, \qquad \dot{\beta}^{\mathcal{A}} \in \partial_{\mathrm{B}^{\mathcal{A}}}\phi^* = \frac{B^{\mathcal{A}}}{\eta^A}$$
$$\dot{M}^{\mathcal{M}} \in \partial_{B^{M^{\mathcal{M}}}}\phi^* = g\left(M^{\mathcal{M}}, \mathrm{B}^{\mathrm{M}^{\mathcal{M}}}\right) \tag{23}$$

Inspired by Kiefer and Lagoudas (2005), function $g\left(M^{\mathcal{M}}, \mathrm{B}^{\mathrm{M}^{\mathcal{M}}}\right)$ is defined in order to describe the magnetization behavior for MFIS. Basically, four critical magnetic field values are assumed: H_{for}^{s} , H_{for}^{f} , H_{rev}^{s} , H_{rev}^{f} , H_0 and H_{max}, denoting start and finish of the forward and reverse magnetic field-induced reorientation process, minimum and maximum applied magnetic field respectively. Based on that, the function is given by:

- **Forward reorientation process $(\dot{H} > 0)$**

$$g = \begin{cases} \dfrac{M^{\mathcal{M}}}{\eta^{\mathrm{H}}}\,, & \text{if } H < H_{for}^{s} \\ \dfrac{-6M^{\mathcal{M}}\left(\mathrm{B}^{\mathrm{M}^{\mathcal{M}}}\right)^3}{\eta^{\mathrm{H}}}, & \text{if } H_{for}^{s} \le H \le H_{for}^{f} \\ 0\,, & \text{if } H < H_{max} \end{cases} \tag{24a}$$

- **Reverse reorientation process $(\dot{H} < 0)$**

$$g = \begin{cases} 0\,, & \text{if } H > H_{rev}^{s} \\ -\dfrac{\mathrm{M}^{\mathcal{M}}}{\eta^{\mathrm{H}}}, & \text{if } H_{rev}^{f} \le H \le H_{rev}^{s} \\ 0\,, & \text{if } H > H_0 \end{cases} \tag{24b}$$

Based on that, a complete set of constitutive equations is obtained.

$$\sigma = E(\varepsilon + \alpha_h^C\beta_2 - \alpha_h^T\beta_1) + \alpha_h^C\beta_2 - \alpha_h^T\beta_1 - \Omega(T - T_0) \tag{25}$$

$$\dot{\beta}^{+} = \frac{\mathrm{B}^{+}}{\eta^{\mathcal{M}}} = \frac{1}{\eta^{\mathcal{M}}}\{\alpha\,\varepsilon + \Lambda_1 + \beta^{-}\left(2\alpha^{\mathrm{h}}\alpha + \mathrm{E}\alpha_{\mathrm{h}}^{2}\right) - \beta^{+}\left(2\alpha^{\mathrm{h}}\alpha + \mathrm{E}\alpha_{\mathrm{h}}^{2}\right) + \alpha^{\mathrm{h}}[\mathrm{E}\varepsilon - \Omega(\mathrm{T}-\mathrm{T}_0)] - \mu_0\mathrm{H}\mathrm{M}^{\mathcal{M}} - \partial_1\mathrm{J}_{\pi}\} \tag{26}$$

$$\dot{\beta}^{-} = \frac{\mathrm{B}^{-}}{\eta^{\mathcal{M}}} = \frac{1}{\eta^{\mathcal{M}}}\{-\alpha\,\varepsilon + \Lambda_2 + \beta^{+}\left(2\alpha^{\mathrm{h}}\alpha + \mathrm{E}\alpha_{\mathrm{h}}^{2}\right) - \beta^{-}\left(2\alpha^{\mathrm{h}}\alpha + \mathrm{E}\alpha_{\mathrm{h}}^{2}\right) - \alpha^{\mathrm{h}}[\mathrm{E}\varepsilon - \Omega(\mathrm{T}-\mathrm{T}_0)] - \mu_0\mathrm{H}\mathrm{M}^{\mathcal{M}} - \partial_2\mathrm{J}_{\pi}\} \tag{27}$$

$$\dot{\beta}^{\mathcal{A}} = \frac{\mathrm{B}^{\mathcal{A}}}{\eta^{\mathcal{A}}} = \frac{1}{\eta^{\mathcal{A}}}\left\{-\frac{1}{2}(\mathrm{E}^{\mathcal{A}} - \mathrm{E}^{\mathrm{M}})\left(\varepsilon + \alpha^{\mathrm{h}}(\beta^{-} - \beta^{+})\right)^{2} + \Lambda_3 + (\Omega^{\mathcal{A}} - \Omega^{\mathcal{M}})(\mathrm{T}-\mathrm{T}_0)\left(+\alpha^{\mathrm{h}}(\beta^{-} - \beta^{+})\right) - \mu_0\mathrm{H}(\mathrm{M}^{\mathcal{A}} - \mathrm{M}^{\mathcal{M}}) - \partial_3\mathrm{J}_{\pi}\right\} \tag{28}$$

$$\dot{M}^{\mathcal{M}} = \frac{g\left(M^{\mathcal{M}}, \mathrm{B}^{\mathrm{M}^{\mathcal{M}}}\right)}{\eta^{\mathrm{H}}} \tag{29}$$

Since the pseudo-potential of dissipation is convex, positive and vanishes at the origin, the Clausius–Duhem inequality is automatically satisfied under the condition that the entropy is defined as $s = -\partial\psi/\partial T$.

In order to take into account differences of the phase transformation kinetics, different parameter values of the dissipation parameters are assumed for loading and unloading behavior:

$$\begin{cases}\eta^{\mathcal{M},\mathcal{A}} = \eta_C^{\mathcal{M},\mathcal{A}} & \text{if} \quad \dot{\varepsilon} > 0 \\ \eta^{\mathcal{M},\mathcal{A}} = \eta_D^{\mathcal{M},\mathcal{A}} & \text{if} \quad \dot{\varepsilon} < 0\end{cases} \tag{30}$$

$$\begin{cases}\eta^{H} = \eta_C^{H} & \text{if} \quad \dot{\mathrm{H}} > 0 \\ \eta^{H} = \eta_D^{H} & \text{if} \quad \dot{\mathrm{H}} < 0\end{cases} \tag{31}$$

3. NUMERICAL RESULTS

This section presents a discussion of the thermo-magneto-mechanical behavior of MSMA predicted by the proposed model where an MSMA specimen subjected to compression is considered. Initially, model parameters are adjusted to magnetic field induced phase transformation (FIPT), by comparing numerical results with experimental results presented by Karaman *et al*. (2006) and Karaca *et al*. (2007). Afterward, model parameters are adjusted to magnetic field induced martensitic variant reorientation (MFIS), using experimental results presented by Tickle (2000) and Heczko (2005) as a reference.

3.1. Thermo-mechanical Phase Transformation

This section deals with thermomechanical behavior of MSMA. Experimental results due to Karaman *et al.* (2006) are used as reference. Basically, pseudo elastic pseudo elastic compressive tests are carried out at four distinct temperatures. Model adjustment is performed at *T*=193K and the others are obtained with the same set. Table 1 presents model parameters and Figure 1 presents a comparison between numerical and experimental results, showing a good agreement.

Table 1: Model parameters adjusted from Karaman's experimental results

$E^{\mathcal{A}}$(GPa)	$E^{\mathcal{M}}$(GPa)	$\Omega^{\mathcal{A}}$(MPa/K)	$\Omega^{\mathcal{M}}$(MPa/K)	α_H (MPa)	α (MPa)
6	12.5	0.74	0.17	0.0245	174
L_0 (MPa)	L (MPa)	$\mathrm{L}_0^{\mathcal{A}}$(MPa)	$\mathrm{L}^{\mathcal{A}}$(MPa)	$\mathrm{T}^{\mathcal{M}}$(K)	$\eta_C^{\mathcal{M}}$ (MPa)
0.26	108	0.93	122	173	0.101
$\eta_D^{\mathcal{M}}$ (MPa)	$\eta_C^{\mathcal{A}}$(MPa)	$\eta_D^{\mathcal{A}}$(MPa)			
0.09999	0.1	0.09999			

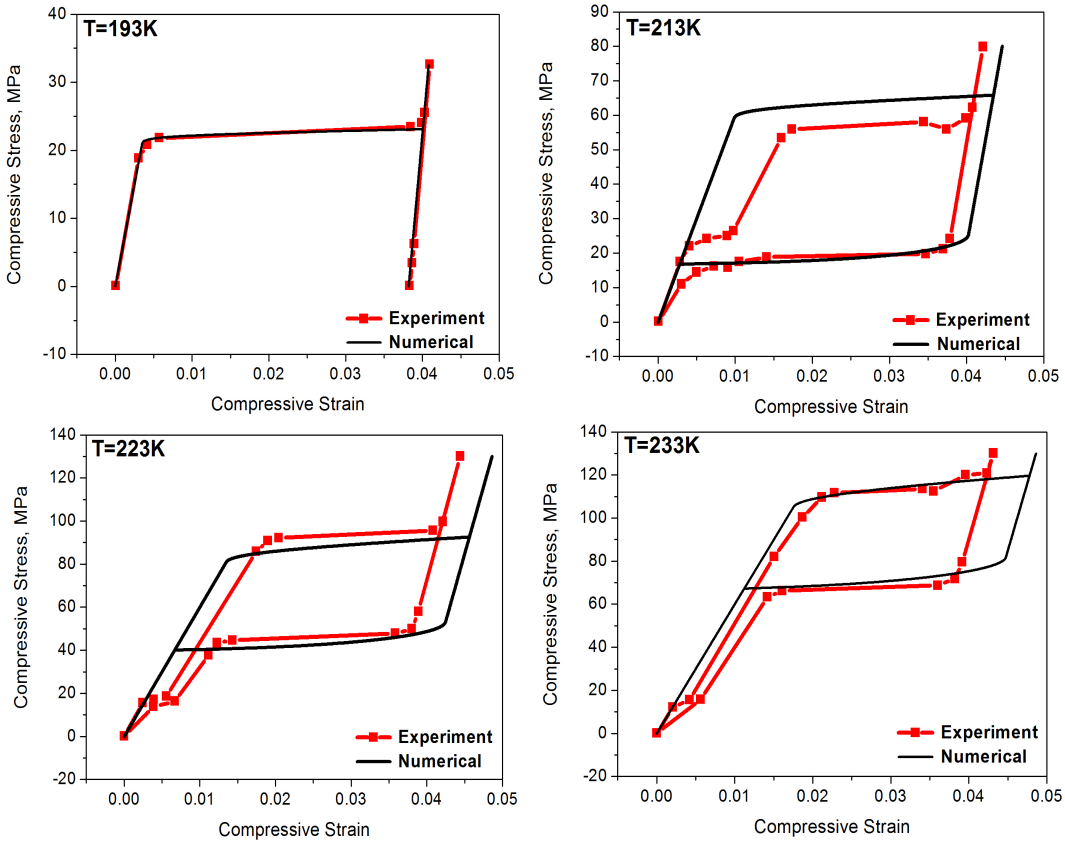

Figure 1: Comparison between numerical and experimental results (Karaman *et al.*, 2006).

3.2. Magneto-mechanical Phase Transformation

The magneto-mechanical calibration of the proposed model is evaluated by comparing the numerical simulations with experimental data presented by Karaca *et al*. (2007), which describes compressive tests on NiMnGa samples.

Table 1 presents model parameters. Figure 2 shows experimental pseudo elastic response at T=213K under zero (blue line) and 1.6 T applied magnetic field (red line), where the difference between the plateau stress levels with and without magnetic field defines the magneto-stress (σ_{mag}). Prior to each stress cycle, external magnetic field is applied along the [011] direction, perpendicular to the loading direction. This value is assumed to be constant during the test. Tests are done under a magnetic induction $(B = 1.6\text{T})$ generated by applying a magnetic field $\text{H} = 620\ \text{KAm}^{-1}$. Figures 3a and 3b establish a comparison between numerical and experimental results at T=213K with and without magnetic field, respectively.

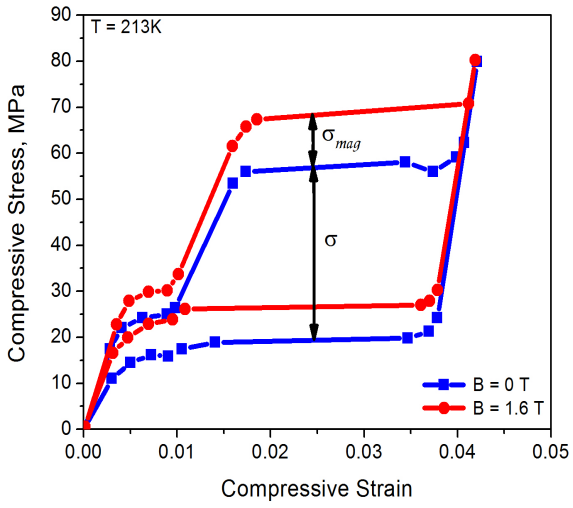

Figure 2: Experimental stress–strain curves (Karaca *et al.*, 2007);

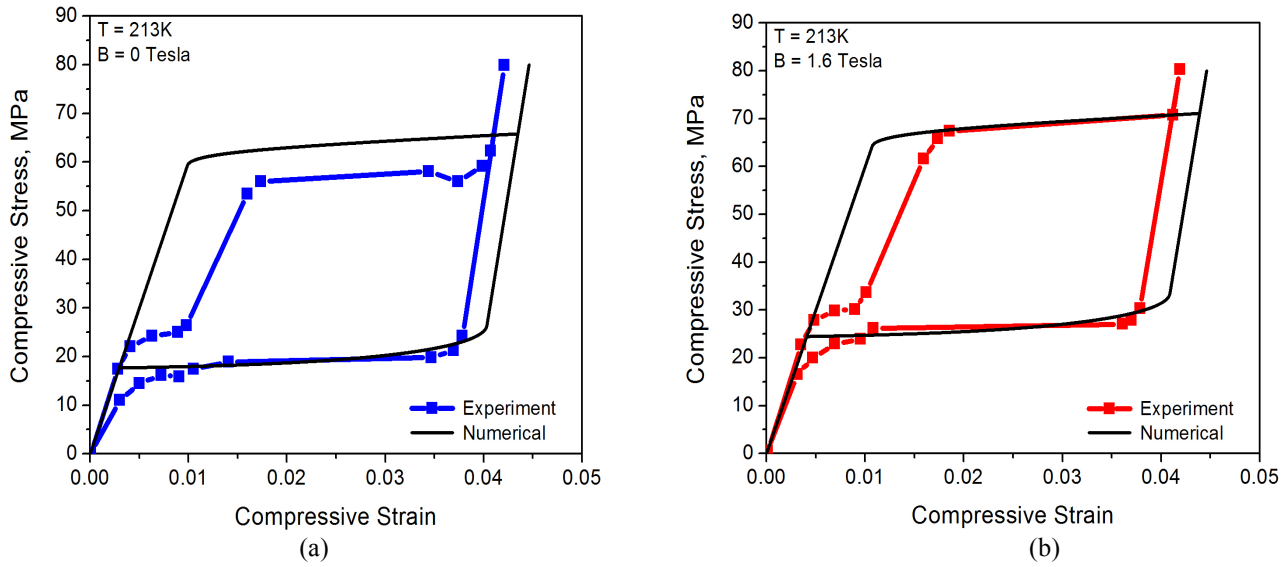

Figure 3: (a) Comparison between numerical and experimental (Karaca *et al*., 2007) results with B=0 T; (b) Comparison between numerical and experimental (Karaca *et al*., 2007) results with B=1.6T.

3.3. Magneto-mechanical Reorientation

This section compares numerical results with experimental data considering magnetic shape memory effect induced in NiMnGa single crystal specimen under the application of an external stress field. Three different stress levels are compared (Tickle, 2000). Model parameters are shown in Tab. 2. Figure 4 presents a comparison between numerical and experimental results at T=183 K. Note that results are showing good agreements.

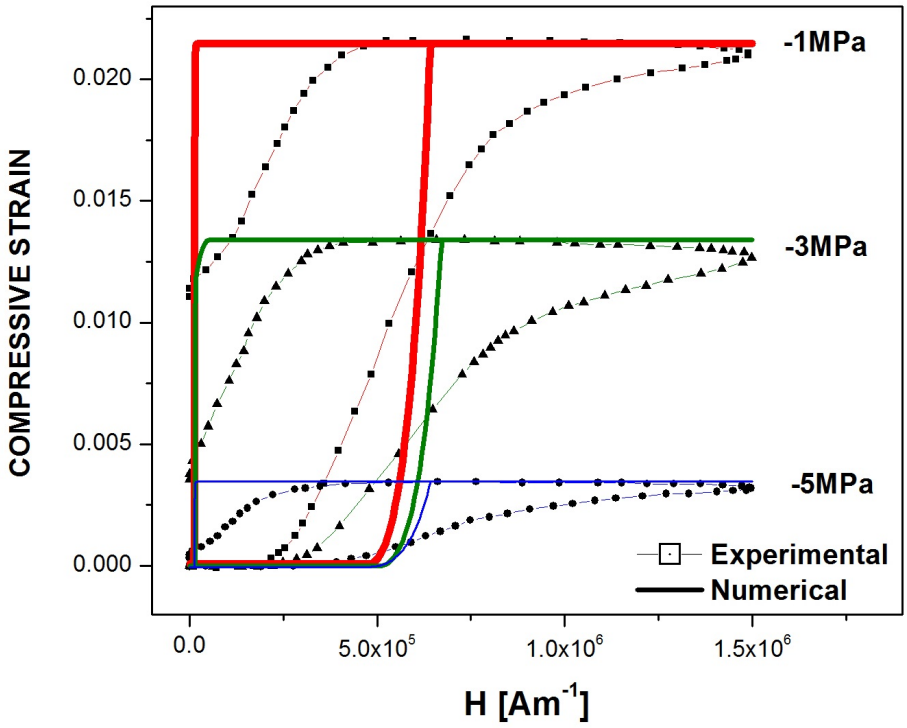

Figure 4: Comparison between numerical and experimental results MFIR (Tickle, 2000).

Table 2: Model parameters adjusted from Tickle's and Heczko's experimental results.

$E^{\mathcal{A}}$ (GPa)	$E^{\mathcal{M}}$ (GPa)	$\Omega^{\mathcal{A}}$ (MPa/K)	$\Omega^{\mathcal{M}}$ (MPa/K)	α^{h} (MPa)	α (MPa)
54	48	0.74	0.17	0.0187	130
L_0 (MPa)	L (MPa)	$L_0^{\mathcal{A}}$ (MPa)	$L^{\mathcal{A}}$ (MPa)	$T^{\mathcal{M}}$ (K)	$\eta_C^{\mathcal{M}}$ (MPa)
100	18	1	1	173	0.1
$\eta_D^{\mathcal{M}}$ (MPa)	$\eta_C^{\mathcal{A}}$ (MPa)	$\eta_D^{\mathcal{A}}$ (MPa)	η_C^{H} (MPa)	η_D^{H} (MPa)	
0.05	1	1	0.0043	0.00119	

3.4. Magnetization

Variant reorientation process provides a mechanism to change material magnetization. For stress levels below the blocking stress, magnetic field-induced changes of the magnetization. In the presence of a magnetic field, microstructural rearrangement is therefore always coupled to a magnetization change. Figure 5 presents a sequence of activation of different mechanisms: Initially, a linear slope of the magnetization curves corresponds to the magnetization of the constrained crystal along the magnetic hard axis. Once the critical field for variant reorientation has been reached, the magnetic field-favored variant $(\mathcal{M})$ nucleates and a sharp change in the slope of the magnetization curves occurs. In the reorientation region, the magnetization change is nonlinear and similar to the evolution of the magnetic field-induced strain observed in the same field regime. At high field values, the stress-favored variant is completely eliminated and the material is magnetically saturated in the field direction. A single variant domain configuration at magnetic saturation is observed. Reverse reorientation follows the same idea. Note that further decrease of the magnetic field completely eliminates variant $(\mathcal{M})$ at the threshold value of H_{rev}^{f}, and for the resulting single compressive detwinned martensite variant $(\mathcal{M}^{-})$.

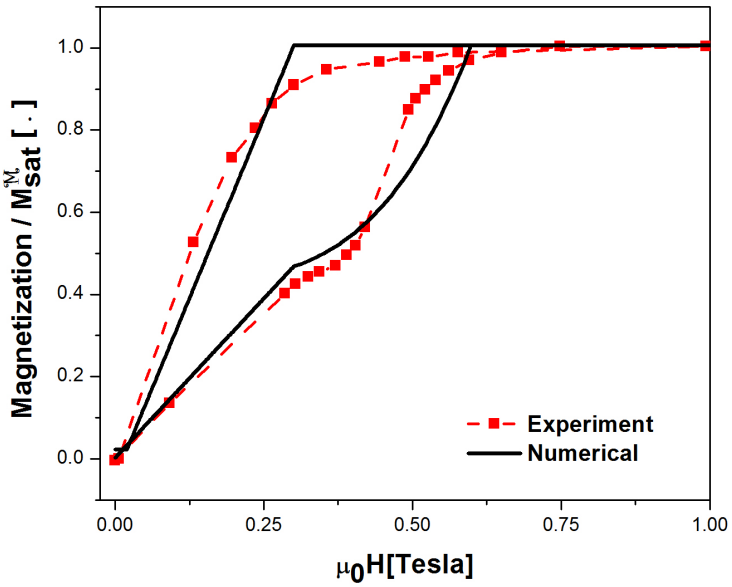

Figure 5: Comparison between numerical and experimental results (Heczko, 2005) of magnetization.

4. CONCLUSIONS

A macroscopic constitutive model is developed to describe the thermo-magneto-mechanical behavior of MSMAs. In essence, magnetic behavior is incorporated on the constitutive model proposed by Paiva *et al*. (2005). The underlying mechanisms are due to austenitic to martensitic phase transformation (FIPT), martensitic variant reorientation (MFIS) and magnetization. In the first one, FIPT, the applied temperature has a strong influence on the pseudoelastic response and the applied magnetic field can increase the critical stress level to start the phase transformations. For the MFIS, it is clear the strong influence of the applied stress on the magneto-mechanical response. The magnetization curve points out the high anisotropy between stress favored variant and field favored variant. For all mechanisms under constant applied stress, a hysteretic behavior takes place by switching on and off the applied magnetic field. Numerical simulations attest that the model captures the general thermo-magneto-mechanical behavior of MSMAs, and model predictions show

good agreement with the experimental data.

5. ACKNOWLEDGEMENTS

The authors would like to acknowledge the support of the Brazilian Research Agencies CNPq, CAPES and FAPERJ and through the INCT-EIE (National Institute of Science and Technology - Smart Structures in Engineering) the CNPq and FAPEMIG. The Air Force Office of Scientific Research (AFOSR) is also acknowledged.

6. REFERENCES

Boyd, J. G., Lagoudas, D. C., 1996. "A thermodynamical constitutive model for shape memory materials. Part I. The monolithic shape memory alloy", International Journal of Plasticity, Vol. 12 (6), 805–842.

Chernenko, V.A., Mullner, P. and Kostorz, G., 2004, "A microscopic approach to the magnetic-field-induced deformation of martensite (magnetoplasticity)", Journal of Magnetism and Magnetic Materials, Vol. 267, pp. 325–334.

Coleman, B.D., Noll, W., 1963. "The thermodynamics of elastic materials with heat conduction and viscosity", Archive for Rational Mechanics and Analysis, Vol. 13, 167–178.

Gauthier, J.Y. *et al*., 2006, "Multistable Actuator Based on Magnetic Shape Memory Alloys", In Proceedings of the Actuator 2006, Bremen, Germany.

Glavatska, N.I., Rudenko, A.A., Glavatskiy, I.N., L'vov, V.A., 2003. "Statistical model of magnetostrain effect in martensite", Journal of Magnetism and Magnetic Materials, Vol. 265 (2), 142–151.

Heczko, O., 2005, " Magnetic shape memory effect and magnetization reversal", Journal of Magnetism and Magnetic Materials, Vol. 290-291 (2), 787-794.

Henry, C.P., Bono, D., Feuchtwanger, J., Allen, S.M., O'handley, R.C., 2002, "AC Field-Induced Actuation of Single Crystal Ni–Mn–Ga", Journal of Applied Physics, Vol. 91, pp. 7810– 7811.

Hirsinger, L., and Lexcellent, C., 2003, "Modelling detwinning of martensite platelets under magnetic and (or) stress actions on NiMnGa alloys", Journal of Magnetism and Magnetic Materials 254–255, pp. 275–277.

James, R.D. and Wuttig, M., 1998, "Magneto Striction of Martensite", Philosophical Magazine, Vol. 77(5), pp. 1273–1299.

Jin, Y.M., 2009, "Domain microstructure evolution in magnetic shape memory alloys: phase-field model and simulation", Acta Mater, Vol. 57, pp. 2488–2495.

Karaca, H.E., Karaman, I., Lagoudas, D.C., *et al*, 2006, "Recoverable Stress Induced Martensitic Transformation in a Magnetic CoNiAl Alloy", Scripta Materialia, Vol. 49, pp. 831–836.

Karaman I. et. al., 2006, "Stress-Assisted Reversible Magnetic Field-Induced Phase Transformation in Ni_2MnGa Magnetic Shape Memory Alloys", Scripta Materialia, 55 (4), pp. 403–406.

Kiefer, B. and Lagoudas, D.C., 2005. "Magnetic Field-Induced Martensitica Variant Reorientation in Magnetic Shape Memory Alloys", Philosophical Magazine, Vol. 85, (33-35), pp. 4289 4329.

Kiefer, B., and Lagoudas, D.C., 2008, "Modeling of the Variant Reorientation in Magnetic Shape-Memory Alloys Under Complex Magneto-mechanical Loading", Materials Science and Engineering, Vol. 481–482, pp.339–342.

Kiefer, B., Karaca, H.E., Lagoudas, D.C., Karaman, I., 2007, "Characterization and Modeling of the Magnetic Field-Induced Strain and Work Output in Ni_2MnGa Shape Memory Alloys", Journal of Magnetism and Magnetic Materials, Vol. 312, pp. 164–175.

Li, L.J., Lei, C.H., Shu, Y.C., Li, J.Y., 2011, "Phase-Field Simulation of Magneto Elastic Couplings in Ferromagnetic Shape Memory Alloys", Acta Materials, Vol. 59, pp. 2648–2655

Likhachev, A.A., Ullakko, K., 2000b. "Quantitative Model of Large Magnetostrain Effect in Ferromagnetic Shape Memory Alloys", The European Physical Journal, Vol. 14 (2), 263–267.

Malvern, L.E., 1969. "Introduction to the Mechanics of a Continuous Medium", Series in Engineering of the Physical Sciences. Prentice Hall.

Müllner, P., Chernenko, V.A., Kostorz, G., 2002. "A Microscopic Approach to the Magnetic-Field-Induced Deformation of Martensite (Magnetoplasticity) ", Journal of Magnetism and Magnetic Materials, Vol. 267, 325–334.

Murray, S.J., Marioni, M., Allen, S.M., O'Handley, R.C., 2000a. "6% Magnetic-Field-Induced Strain by Twin-Boundary Motion in Ferromagnetic Ni-Mn-Ga", Applied Physics Letters, Vol. 77 (6), 886–888.

O'Handley, R.C., 1998. "Model For Strain and Magnetization in Magnetic Shape-Memory Alloys", Journal of Applied Physics, Vol. 83 (6), 3263–3270.

Ortiz, L.A., Scott, R.F. and Lee, J., 1983, "Dynamic Centrifuge Testing of a Cantilever Retaining Wall", Earthquake Engineering and Structural Dynamics, Vol. 11, pp. 251-268

Paiva, A. and Savi, M. A., 2005, "A Constitutive Model for Shape Memory Alloys Considering Tensile–Compressive Asymmetry and Plasticity", International Journal of Solids and Structures, Vol. 42, pp. 3439–3457.

Paiva, A., Savi, M. A., Braga, A. M. B. and Pacheco, P. M. C. L., 2005, "A Constitutive Model for Shape Memory Alloys Considering Tensile-Compressive Asymmetry and Plasticity", International Journal of Solids and Structures, Vol. 42, n. 11-12, pp. 3439-3457.

Qidwai, M.A., Lagoudas, D.C., 2000a. “Numerical Impementation of a Shape Memory Alloy Thermomechanical Constitutive Model Using Return Mapping Algorithms”, International Journal for Numerical Methods in Engineering, Vol. 47, pp. 1123–1168.

Tan, H. and Elahinia, M.H., 2008, “A Nonlinear Model for Ferromagnetic Shape Memory Alloy Actuators”, Communications in Nonlinear Science and Numerical simulations, Vol. 13, pp. 1917–1928.

Tickle, R., 1999. “Ferromagnetic shape memory materials”, Ph.D. thesis, University of Minnesota.

Tickle, R., James, R.D., 1999. “Magnetic and Magnetomechanical Properties of Ni_2MnGa”, Journal of Magnetism and Magnetic Materials, Vol. 195 (3), pp. 627–638.

Ullakko, K., Huang, J.K., Kantner, C., O’Handley, R.C., Kokorin, V.V., 1996. “Large Magnetic-Field-Induced Strains in Ni_2MnGa Single Crystals”, Applied Physics Letters, Vol. 69 (13), pp. 1966–1968.

7. RESPONSIBILITY NOTICE

The authors are the only responsible for the printed material included in this paper.